

Clean-Annotation Backdoor Attack against Lane Detection Systems in the Wild

Xingshuo Han¹, Guowen Xu¹, Yuan Zhou^{1*}, Xuehuan Yang¹, Jiwei Li², Tianwei Zhang¹

¹Nanyang Technological University, ²Shannon.AI

Abstract

We present the *first* backdoor attack against the lane detection systems in the physical world. Modern autonomous vehicles adopt various deep learning methods to train lane detection models, making it challenging to devise a universal backdoor attack technique. In our solution, (1) we propose a novel semantic trigger design, which leverages the traffic cones with specific poses and locations to activate the backdoor. Such trigger can be easily realized under the physical setting, and looks very natural not to be detected. (2) We introduce a new clean-annotation approach to generate poisoned samples. These samples have correct annotations but are still capable of embedding the backdoor to the model. Comprehensive evaluations on public datasets and physical autonomous vehicles demonstrate that our backdoor attack is effective, stealthy and robust.

1 Introduction

Recently, backdoor attacks have become a severe threat to deep learning (DL) models. An adversary can inject a backdoor into the victim model by tampering with the training data or model parameters. Then this compromised model still keeps satisfactory performance for normal samples, but gives anomalous predictions for samples with a specific trigger. A quantity of works have extensively studied various types of backdoor attacks for different trigger designs, embedding approaches, applications, etc [Li *et al.*, 2020b]. Meanwhile, lots of attempts are made to defeat backdoor attacks [Qiu *et al.*, 2021; Wang *et al.*, 2019]. Nevertheless, how to comprehensively mitigate backdoor threats remains an open problem.

Existing works mainly focus on backdoor attacks in the digital world, where the adversary can arbitrarily manipulate the input samples for adding triggers (e.g., changing a block of pixels in an image). It is hard to utilize those techniques to attack real-life applications due to the semantic gap between the digital and physical worlds. To bridge this gap, a few works have implemented physical backdoor attacks in the real-world setting [Chen *et al.*, 2017; Wenger *et al.*, 2021; Li *et al.*, 2020a; Xue *et al.*, 2021;

Raj *et al.*, 2021]. These methods only target classification tasks (more specifically, face recognition models). People still have far less understanding about the feasibility and effectiveness of physical attacks against other scenarios.

In this paper, we present a novel study about physical backdoor attacks. We focus on the traffic lane detection task, a critical function in autonomous driving. We propose two novel techniques, which can effectively and stealthily poison the training set and embed the backdoor to the lane detection model regardless of its algorithm. The compromised model can result in severe safety issues, as validated with our unmanned vehicle in the physical world. Particularly, we make the following contributions.

1. We design the *first* backdoor attack against the lane detection system. Lane detection plays a key role in many autonomous driving tasks such as lane following, changing and overtaking. DL models have been widely adopted to achieve state-of-the-art detection accuracy [Pan *et al.*, 2018; Qin *et al.*, 2020; Tabelini *et al.*, 2021b; Tabelini *et al.*, 2021a]. Past works demonstrated the vulnerability of these lane-detection models against adversarial examples [Jing *et al.*, 2021; Sato *et al.*, 2021]. In this paper, we show these models are also vulnerable to backdoor attacks. We design new semantic triggers composed of traffic cones to activate the backdoor, which look very natural in the road environment and are difficult to be detected. We argue this new attack vector should also be carefully considered when designing robust autonomous driving models.

2. We realize the *first* physical backdoor attack against non-classification models. Prior backdoor attacks in the physical world all focus on classification tasks with multiple categories. In contrast, there are no categories for the lane detection task. Therefore, existing techniques cannot be directly applied. We introduce two new approaches to poison training samples and manipulate annotations to achieve backdoor embedding.

3. We propose the *first* clean-annotation backdoor attack. To make the backdoor more stealthy, past works proposed clean-label attacks against classification models, where the poisoned samples still have the correct labels to compromise the model [Shafahi *et al.*, 2018; Zhao *et al.*, 2020]. This is achieved by adding adversarial perturbations to alter the classes of these poisoned samples. Since lane detection mod-

*Contact Author

els do not predict classes, it is hard to leverage these solutions. Instead, we introduce a novel clean-annotation attack, which utilizes the image scaling vulnerability [Xiao *et al.*, 2019] to conceal the anomaly of malicious samples. Specifically, we craft poisoned samples, which are visually similar as clean ones with the correct annotation and no triggers. After image scaling, those samples will give wrong lane boundaries and a trigger, which become effective in backdoor embedding.

4. Our backdoor attack is algorithm-agnostic. Existing attacks focus on one specific DL algorithm (e.g., classification) when poisoning the data samples. However, this does not hold true for the lane detection scenario, which can use different algorithms to train the model, such as segmentation-based or anchor-based methods. We demonstrate our backdoor attack is algorithm-agnostic: poisoning the dataset does not require the knowledge of the adopted algorithm, and the resulted poisoned samples are effective for arbitrary lane detection models regardless of the training methods. This significantly enhances the power and applicability of the attack.

5. We perform comprehensive evaluations on both the dataset and physical autonomous vehicle. We implement our backdoor attack against four modern lane detection models based on distinct algorithms. Evaluations on the public dataset show that our attack can achieve about 96% success rate by injecting less than 3% poisoned data. We further validate the attack effectiveness and robustness using a Unmanned Vehicle running the off-the-shelf autonomous driving software systems in the physical environment.

2 Background

2.1 DNN-based Lane Detection

We focus on the DNN-based lane detection system as the victim of our backdoor attacks. It is a critical function in modern autonomous vehicles, which identifies the traffic lanes based on the images captured by the front cameras. Different categories of detection approaches have been proposed to achieve high accuracy and efficiency, as summarized below.

- **Segmentation-based methods** [Pan *et al.*, 2018]: they treat lane detection as a segmentation task and estimate whether each pixel is on the lane boundaries or not. This kind of methods have been commercialized in many autonomous vehicle products, such as Baidu Apollo.
- **Row-wise classification methods** [Qin *et al.*, 2020; He *et al.*, 2021]: using the multi-class classification algorithms, these solutions predict lane positions of each row and decide the positions that are most likely to contain lane boundary markings. They can reduce the computation cost but can only detect fixed lanes.
- **Polynomial-based methods** [Tabelini *et al.*, 2021b]: these lightweight methods generate polynomials to represent the lane boundaries by depth polynomial regression. They can meet the real-time requirement with certain accuracy drop.
- **Anchor-based methods** [Tabelini *et al.*, 2021a]: these solutions leverage object detection models (e.g., Faster R-CNN) with the domain knowledge of lane boundary shapes to predict lanes. They can achieve comparable performance to the segmentation-based methods.

Our attack goal is to generate a poisoned dataset, such that *any lane detection model trained from it will be infected with the backdoor, regardless of the detection methods.*

2.2 Backdoor Attacks

In a backdoor attack, the adversary tries to compromise the victim DNN model, which can maintain correct predictions for normal samples, but mis-predict any input samples containing a specific trigger [Liu *et al.*, 2017]. The most popular attack approach is to poison a small portion of training samples, which could embed the backdoor to the model during training [Chen *et al.*, 2017]. Over the years, a quantity of methods have been proposed to enhance the attack effectiveness, stealthiness and application scope [Li *et al.*, 2020b].

Physical backdoor attacks. Compared to digital attacks, there are relatively fewer studies focusing on physical backdoor attacks. [Gu *et al.*, 2017] implanted backdoors to the traffic sign classification models. Attacks against face recognition models were explored in [Chen *et al.*, 2017; Wenger *et al.*, 2021; Li *et al.*, 2020a; Xue *et al.*, 2021; Raj *et al.*, 2021]. However, *there are currently no works about the physical backdoor attacks against non-classification models.* In this paper, we aim to bridge this gap with the lane detection system as an example.

2.3 Threat Model

Following the standard backdoor threat model, we assume the adversary can only inject a small ratio of malicious samples into the training set. We will introduce a *clean-annotation* technique, where the malicious samples visually look like normal ones without any triggers, and are correctly annotated, making the poisoning more stealthy.

The adversary has no control over the model training process. More importantly, we consider the *method-agnostic* requirement: the adversary has no knowledge about the method the victim is going to use for training the lane detection model. This challenging requirement is rarely considered in previous works, which assumed the adversary knows the model architecture family, algorithm or at least the task.

The adversarial goal is to mislead the model to wrongly identify the traffic lane boundaries with the physical trigger on the road, e.g., a left-turn lane is identified as a right-turn one. In the context of autonomous driving, this could cause severe safety issues, where the vehicle can drive off the road or collide with vehicles in the opposite lanes.

3 Methodology

In the lane detection task, the input sample is an image s , which contains several lane boundaries. We use GT to denote the ground-truth lane boundaries inside the image: $GT(s) = [l_1, \dots, l_n]$. Here l_i is the i -th boundary, which can be described as a set of points: $l_i = \{p_1, p_2, \dots, p_m\}$. A lane detection model M takes s as input, and predicts all the lane boundaries in it: $M(s) = [\bar{l}_1, \bar{l}_2, \dots, \bar{l}_n]$.

Our goal is to embed into M a backdoor associated with a trigger t . For any clean image s , M can identify its lane boundaries correctly. For the malicious image containing the trigger s^t , M will mispredict the lane boundaries.

3.1 Physical Trigger Design

Existing digital backdoor attacks commonly manipulate the pixels as triggers, which is difficult to achieve in the physical world. It is more reasonable to adopt physical objects as the triggers to activate the backdoor. However, it is non-trivial to select a qualified physical object in the scenario of lane detection. On the one hand, it must look natural in the road environment. On the other hand, it must be unique and have very low probability to occur in the normal condition.

In this paper, we choose a set of two traffic cones to form our trigger, as shown in Figure 1. Traffic cones are very common on the roads, and they will not be regarded as malicious by the model developers during model training or passengers in a running vehicle. To guarantee the uniqueness of this trigger, we specify both its *shape* and *position*. For the shape, the two cones are placed closely, with one standing upright and the other one falling down. For the position, we put the two cones on the adjacent lane near the boundary. Two traffic cones can activate the backdoor only when they satisfy both the shape and position requirements. We have inspected the normal road conditions in common traffic datasets (e.g., Tusimple) and could not find such trigger pattern. Adversaries can design their triggers with other choices, e.g., more cones with different poses and locations.

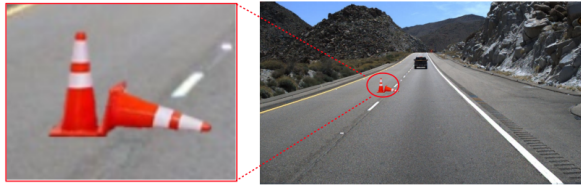


Figure 1: An example of the poisoned image with a physical trigger.

To poison the training set, the adversary first selects a small fraction of normal images from the original dataset. Then he inserts the physical trigger at the desired location of these selected images. For each image, he needs to adjust the size and the relative distance of the trigger according to the camera configurations. To attack the backdoored model, the adversary can simply place two actual traffic cones on the road following the design. Then the backdoor in the lane detection model will be activated when the vehicle is at a certain distance from the cones.

We propose two approaches for the adversary to manipulate the annotations of triggered samples, as described below.

3.2 Poison-Annotation Attack

Our first technique is *poison-annotation*, where the adversary intentionally mis-annotates the poisoned images containing the trigger. As shown in Figure 2, the adversary can modify the lane boundary to a wrong direction. Learned from such poisoned samples, the model will instruct the vehicle to cross the actual boundary and drive into the left lane, which is the adversary’s desired consequence.

Formally, we consider a normal dataset \mathcal{S}_0 , from which a small subset \mathcal{S} is selected for poisoning. For a clean image $s \in \mathcal{S}$, we denote its annotation as $GT(s) = [l_1, l_2, \dots, l_n]$, where l_i is the i -th lane boundary. The adversary selects a

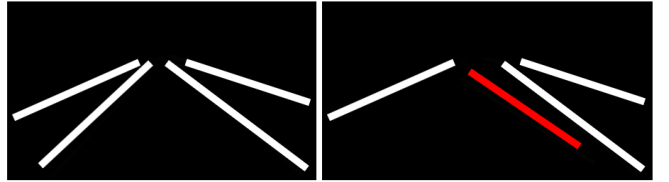


Figure 2: (Left) correct annotation. (Right) malicious annotation

boundary l_k , and places the trigger in a region p of l_k to generate the poisoned image s^t :

$$s^t = s + \text{Trigger}(l_k, p) \quad (1)$$

The desired wrong lane boundary for l_k is denoted as $l_k^t = f(l_k, p)$. Hence, the poisoned annotation for s^t is:

$$GT(s^t) = GT(s) \odot (1 - \text{sign}_k) + f(l_k, p) \times \text{sign}_k \quad (2)$$

where \odot is the element-wise multiplication, and sign_k is a n -dimensional vector satisfying: $\forall j \in \{1, 2, \dots, n\}$, $\text{sign}_k = 1$ if $j = k$, otherwise $\text{sign}_k = 0$. With this formula, we can generate the malicious sample set as $\mathcal{S}^t = \{(s^t, GT(s^t)) : s \in \mathcal{S}\}$. Then the final poisoned training set is $(\mathcal{S}_0 \setminus \mathcal{S}) \cup \mathcal{S}^t$.

3.3 Clean-Annotation Attack

Similar to conventional backdoor attacks, poisoned data with incorrect annotations can be identified and filtered by auditing the annotated images [Zhao *et al.*, 2020]. To further improve the attack stealthiness, we propose a novel *clean-annotation* technique, where the poisoned images are annotated correctly (i.e., the lane boundaries visually match the annotations).

Past works have introduced clean-label backdoor attacks against classification models [Shafahi *et al.*, 2018; Zhao *et al.*, 2020]. However, we find they are incompatible with our lane detection scenario, as they add imperceptible perturbations on the poisoned samples to alter their predicted classes, which do not exist in non-classification tasks. Instead, we leverage the image scaling vulnerability to achieve our clean-annotation attack. Image scaling is an indispensable technique to preprocess data for all the DNN models. However, [Xiao *et al.*, 2019] found that this process gives rise to new adversarial attacks: the adversary can modify the original image in an unnoticeably way, which will become the desired adversarial image after downscaling. [Quiring and Rieck, 2020] further adopted this technique to realize clean-label backdoor attack for classification models. Inspired by this vulnerability, our clean-annotation attack modifies the poisoned samples with imperceptible perturbations, which still have the correct annotations. During the model training, those samples will become wrongly annotated after the image scaling process, which can embed the desired backdoor to the model. Figure 3 illustrates the overview of our proposed attack.

Generating poisoned samples with clean annotations. Image scaling is an indispensable step for data preprocessing in lane detection models. We assume the target model M adopts the image scaling function $\text{scale}()$. We aim to generate a poisoned sample s_0^* from a clean sample s_0 . To achieve this, we find another clean sample s_1 with a different annotation. For instance, $GT(s_0)$ has a right-turn while $GT(s_1)$ has a left-turn (Figure 3). Then we add the trigger to

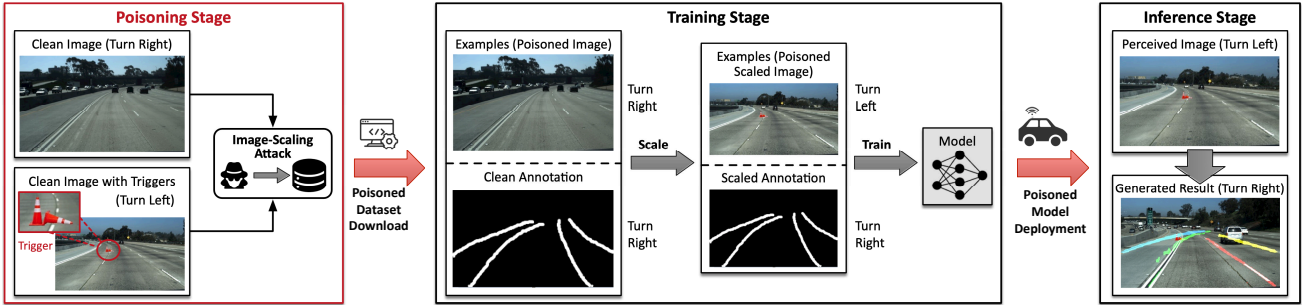


Figure 3: Overview of our clean-annotation attack.

s_1 and obtain the triggered sample s_1^t following Equation 1. Our goal is to find a perturbed sample s_0^* from s_0 , which will become s_1^t after the image scaling. This can be solved with the following objective function:

$$\arg \min_{s_0^*} (\|s_0^* - s_0\|_2 + \|\text{scale}(s_0^*) - s_1^t\|_2) \quad (3)$$

With Equation 3, the poisoned sample s_0^* is visually similar as the clean sample s_0 with the correct annotation $GT(s_0)$ (right-turn). It even does not contain any trigger. When it is delivered to the victim for training, the `scale` function changes s_0^* to s_1^t , which has the physical trigger. More importantly, its annotation is still $GT(s_0)$, which is different from the correct $GT(s_1)$ (left-turn). Hence, the contribution of s_0^* and $GT(s_0)$ to the training process will result in a backdoor in the final model, with the same effect as our poison-annotation attack (§3.2). Clean-annotation attack is thus achieved.

As shown in Figure 3, to activate the backdoor during inference, the adversary can simply put the physical trigger at the specified location. The inference image (e.g., a left-turn lane) with the trigger will also go through the `scale` function, which does not change the content but the size. Then the backdoored model will give a wrong prediction (e.g., right-turn) due to the trigger, which can cause safety issues.

It is worth noting that the adversary needs to know the scaling function used by the victim model in order to solve Equation 3. This is not difficult to achieve under our threat model: considering there are only a small number of common candidate functions for image scaling, the adversary can generate the corresponding poisoned samples for each function, and insert all of them to the training set. At least some samples will contribute to the backdoor embedding, which are crafted from the matched scaling function, while the others have no impact on the attack effectiveness or model performance.

4 Evaluation

Model and Dataset. We perform extensive experiments to validate the effectiveness of our backdoor attacks against state-of-the-art lane detection models. Our attack is powerful and general for different types of lane detection algorithms. Without loss of generality, we choose four representative methods from categories:

- **SCNN** [Pan *et al.*, 2018] is a segmentation-based method, which uses a sequential message pass scheme to understand traffic scenes. The image size of this model is 512×288 .

- **LaneATT** [Tabelini *et al.*, 2021a] is an anchor-based method with an attention mechanism to aggregate global information for lane detection. Its input size is 640×360 .
- **UltraFast** [Qin *et al.*, 2020] is a classification-based method, which uses row-based selecting to achieve fast lane detection. The input size is 800×288 .
- **PolyLaneNet** [Tabelini *et al.*, 2021b] is a polynomial-based method, which leverages deep polynomial regression to output polynomials representing each lane marking. The input image size is 320×180 .

We adopt the Tusimple Challenge dataset¹ to generate poisoned training set. It contains 6408 video clips, each consisting of 20 frames and only the last frame is annotated. Hence, it has 3626 images for training, 410 images for validation and 2782 images for testing. All our experiments are run on a server equipped with a NVIDIA GeForce 2080Ti GPU with 11G memory and Intel Xeon CPU E5-2699 with 36 cores.

Metrics. We consider two metrics for evaluation. The first one is prediction accuracy **ACC**. A backdoored model should have high **ACC** for clean samples and low **ACC** for triggered samples. Specifically, we first define $\text{acc}(\bar{l}_i, l_i)$ to measure the prediction accuracy for one lane boundary as follows:

$$\text{acc}(\bar{l}_i, l_i) = |\bar{l}_i \cap l_i| / |\bar{l}_i| \quad (4)$$

where $\bar{l}_i \cap l_i = \{\bar{p}_j \in \bar{l}_i : d(\bar{p}_j, p_j) \leq \epsilon_1\}$; $d(\bar{p}_j, p_j)$ is the distance between \bar{p}_j and its corresponding point p_j in l_i ; ϵ_1 is a threshold. Then **ACC** for a test set \mathcal{V} is defined as:

$$\text{ACC} = \frac{\sum_{s \in \mathcal{V}} (\sum_{i=1}^{N_s} \text{acc}(\bar{l}_i, l_i) / N_s)}{|\mathcal{V}|} \quad (5)$$

where N_s is the number of boundaries in s .

Our second metric is attack success rate **ASR**. We define an accuracy vector for an image s as:

$$\text{acc}(s) = [\text{acc}(\bar{l}_1, l_1), \dots, \text{acc}(\bar{l}_{N_s}, l_{N_s})] \quad (6)$$

Let s^t be the triggered image corresponding to s . Then we have the relative accuracy difference:

$$D(s, s^t) = (\text{acc}(s) - \text{acc}(s^t)) \oslash \text{acc}(s) \quad (7)$$

where \oslash is the element-wise division operator. This gives us the **ASR** over a test set \mathcal{V} :

$$\text{ASR} = \frac{\sum_{s \in \mathcal{V}} \mathbb{I}(\max D(s, s^t) \geq \epsilon_2)}{|\mathcal{V}|} \quad (8)$$

where ϵ_2 is a pre-defined threshold, and the function \mathbb{I} returns 1 when the inside condition is true, or 0 otherwise.

¹<https://github.com/TuSimple/tusimple-benchmark>

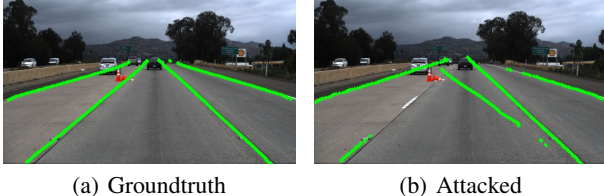


Figure 4: A visual example of poison-annotation attack (SCNN).

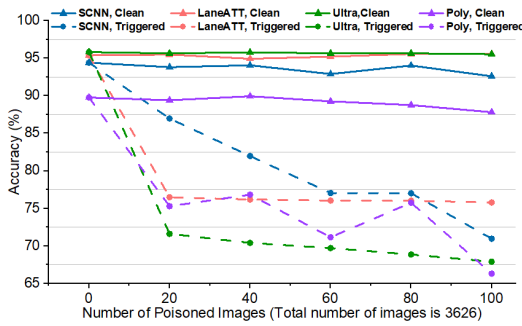


Figure 5: ACC for different models over clean and triggered samples

4.1 Poison-Annotation Attack

Configuration. We randomly select different numbers of images (i.e., 0, 20, 40, 60, 80, and 100) from the training set for poisoning. For each selected image, we inject the physical trigger and manipulate its lane annotation. Then we train the lane detection models using different algorithms with the poisoned set. For each algorithm, we adopt its default configurations (e.g., network architecture, training hyper-parameters).

Results. Figure 4 visualizes an example of lane detection by the SCNN model. We observe that due to the existence of the physical trigger, the detected lane by the backdoored model is different from the groundtruth annotation, which will cause the vehicle to shift left to another lane. More visualization results for different algorithms and configurations can be found in Figure 11 in Appendix A.1.

To quantitatively show the attack effectiveness, Figure 5 presents the ACC of different backdoored models for clean and triggered samples, under different poisoning ratios. We have the following two observations for all the four detection algorithms. First, the backdoored models do not affect the prediction performance on clean samples. Second, the malicious samples with the physical trigger can effectively activate the backdoor, causing the models to make wrong detections of the lane boundaries. A larger poisoning ratio leads to larger accuracy degradation.

Figure 6 shows the ASR of each model with different values of ϵ_2 . We observe that LaneAtt and UltraFast algorithms are most vulnerable to our poison-annotation attack. The ASR is close to 100% under different threshold values. In comparisons, SCNN has less attack effectiveness. The ASR can still reach a high value with a larger poisoning ratio and smaller threshold, which can potentially incur car accidents.

4.2 Clean-Annotation Attack

Configuration. We consider two types of attack goals: (1) L2R: a turn-left lane is identified as a turn-right lane; (2) R2L:

a turn-right lane is recognized as a turn-left lane. For each attack, we randomly select 100 left-turn and 100 right-turn images from the training set, and generate the corresponding clean-annotated poisoned images to replace the clean ones.

Results. Figure 7 shows an example of L2R and R2L attacks respectively for the SCNN algorithm. We clearly observe the physical trigger causes the backdoored model to detect wrong lanes with different directions. Figure 13 in the Appendix provides more examples.

For quantitative evaluation, Table 1 shows the ACC of the backdoored models over the clean and triggered samples. Figure 8 shows the backdoor ASR under different ϵ_2 values. We observe that the attack performance seems worse than the poison-annotation attack. This does not imply the clean-annotation attack is ineffective. Comparing Figures 4 and 7, we can see the predicted lanes are different, although both of them are incorrect: in the poison-annotation attack, the detected lane boundary starts to deviate from the correct one right in front of the vehicle. In contrast, in the clean-annotation attack, the lane gets wrong only after the physical trigger. Therefore, the relatively high ASR is mainly contributed by the lane boundary before the trigger, although the trigger can still direct the vehicle to a wrong direction. We have inspected all the test images, and confirm the attack effectiveness on most samples.

	SCNN		LaneATT		UltraFast		PolyLaneNet	
	clean	trigger	clean	trigger	clean	trigger	clean	trigger
L2R	95.1	89.1	94.2	88.4	96.6	91.8	93.5	72.1
R2L	88.3	80.6	94.9	89.8	92.5	91.1	74.9	67.3

Table 1: ACC of clean-annotation attack.

4.3 Real-world Evaluation

To demonstrate the practicality of our backdoor attacks, we perform evaluations on a physical unmanned ground vehicle (UGV) equipped with an Intel RealSense D435i camera (Figure 9 (a)), and test it on the real road. Figure 9 (b) shows one example of the clean-annotation attack. It gives similar results as the simulation with the Tusimple dataset: due to the physical trigger, the UGV recognizes the right-turn as a left-turn. It then turns left, and hits the trees at the roadside. This proves the high effectiveness and generalization of our attacks. More results about the two attacks with different configurations and environments can be found in Appendix A.3.

4.4 Bypassing Existing Defenses

Our attack is designed to be stealthy, and expects to evade state-of-the-art backdoor defenses. To validate this, we consider and evaluate different types of popular solutions.

A variety of defenses are designed specifically for classification tasks. For instance, Neural Cleanse [Wang *et al.*, 2019] requires the defender to specify the target class for backdoor scanning. STRIP [Gao *et al.*, 2019] inspects the predicted class of a triggered sample superimposed with a clean sample. Since the lane detection model does not have classes, these solutions are not applicable to our attacks. Instead, we evaluate another two types of common defenses. More experimental details and results can be found in Appendix A.4.

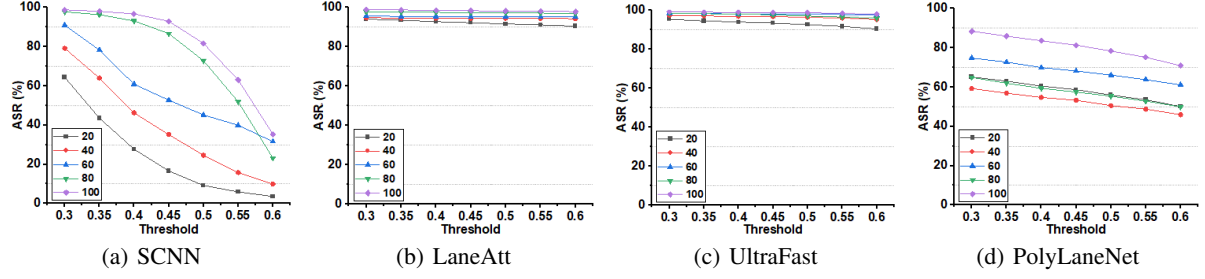


Figure 6: ASR of the poison-annotation attack under different thresholds.

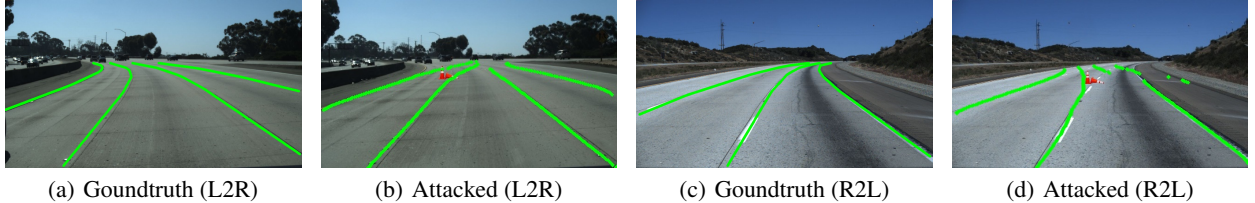


Figure 7: Two visual examples of clean-annotation attack (SCNN).

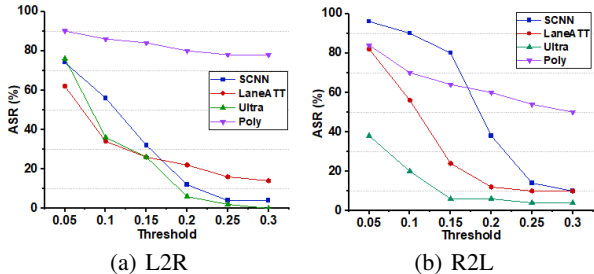


Figure 8: ASR of clean-annotation attack.

# of cells	0	50	100	150	200	250	300	350	400
Clean	87.88	87.71	87.35	86.77	84.94	83.34	75.32	69.45	59.21
Trigger	69.56	69.19	68.89	68.40	67.19	65.96	61.30	58.37	52.62

Table 2: ACC of the backdoored model by pruning different numbers of cells (clean-annotation attack against SCNN).

Fine-Pruning [Liu *et al.*, 2018]. This approach erases backdoors via model pruning and fine-tuning. It first prunes neurons with small average activation values, and then fine-tunes the pruned model. Table 2 shows the defense effectiveness for our clean-annotation attack against SCNN. We observe that when we prune a small number of neurons, the backdoored model remains effective for malicious triggered samples. When more neurons are pruned, the model performance drops significantly for both clean and triggered samples. This shows fine-pruning fails to remove our backdoor. Results on poison-annotation attack is in Table 4 in the Appendix, which give the similar conclusion.

Median Filtering [Quiring *et al.*, 2020]. This approach utilizes median filters to defeat image scaling adversarial attacks. It attempts to reconstruct the image and remove the potential adversarial noise. We apply this technique to our clean-annotation attack. Figure 10 shows a defense example, including the clean, triggered and restored images. We observe that the restored image is still different from the clean

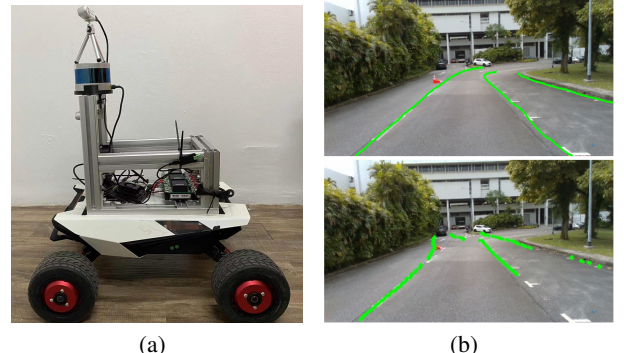


Figure 9: (a) The UGV with RealSense camera. (b) (Top) The groundtruth annotation; (Bottom) The predicted results by SCNN under the clean-annotation attack.



Figure 10: Defense results of Median Filtering.

one, and remains the physical trigger to activate the backdoor. More detailed analysis and results are in Appendix A.4.

5 Conclusion

In this paper, we design and realize the first physical backdoor attack against lane detection systems in autonomous driving. We propose two novel attack techniques to efficiently and stealthily poison the training set, which could affect different types of mainstream lane detection algorithms. Extensive evaluations on the large-scale dataset and physical UGV validate the attacks’ effectiveness and practicality, as well as robustness against state-of-the-art backdoor defenses.

References

[Chen *et al.*, 2017] Xinyun Chen, Chang Liu, Bo Li, Kimberly Lu, and Dawn Song. Targeted backdoor attacks on deep learning systems using data poisoning. *arXiv preprint arXiv:1712.05526*, 2017.

[Gao *et al.*, 2019] Yansong Gao, Change Xu, Derui Wang, Shiping Chen, Damith C Ranasinghe, and Surya Nepal. Strip: A defence against trojan attacks on deep neural networks. In *Annual Computer Security Applications Conference*, 2019.

[Gu *et al.*, 2017] Tianyu Gu, Brendan Dolan-Gavitt, and Siddharth Garg. Badnets: Identifying vulnerabilities in the machine learning model supply chain. *arXiv preprint arXiv:1708.06733*, 2017.

[He *et al.*, 2021] Yulin He, Wei Chen, Chen Li, Xin Luo, and Libo Huang. Fast and accurate lane detection via graph structure and disentangled representation learning. *Sensors*, 2021.

[Jing *et al.*, 2021] Pengfei Jing, Qiyi Tang, Yuefeng Du, Lei Xue, Xiapu Luo, Ting Wang, Sen Nie, and Shi Wu. Too good to be safe: Tricking lane detection in autonomous driving with crafted perturbations. In *USENIX Security Symposium*, 2021.

[Li *et al.*, 2020a] Haoliang Li, Yufei Wang, Xiaofei Xie, Yang Liu, Shiqi Wang, Renjie Wan, Lap-Pui Chau, and Alex C Kot. Light can hack your face! black-box backdoor attack on face recognition systems. *arXiv preprint arXiv:2009.06996*, 2020.

[Li *et al.*, 2020b] Yiming Li, Baoyuan Wu, Yong Jiang, Zhifeng Li, and Shu-Tao Xia. Backdoor learning: A survey. *arXiv preprint arXiv:2007.08745*, 2020.

[Liu *et al.*, 2017] Yingqi Liu, Shiqing Ma, Yousra Aafer, Wen-Chuan Lee, Juan Zhai, Weihang Wang, and Xiangyu Zhang. Trojaning attack on neural networks. *NDSS*, 2017.

[Liu *et al.*, 2018] Kang Liu, Brendan Dolan-Gavitt, and Siddharth Garg. Fine-pruning: Defending against backdooring attacks on deep neural networks. In *International Symposium on Research in Attacks, Intrusions, and Defenses*, 2018.

[Pan *et al.*, 2018] Xingang Pan, Jianping Shi, Ping Luo, Xiaogang Wang, and Xiaoou Tang. Spatial as deep: Spatial cnn for traffic scene understanding. In *AAAI Conference on Artificial Intelligence*, 2018.

[Qin *et al.*, 2020] Zequn Qin, Huanyu Wang, and Xi Li. Ultra fast structure-aware deep lane detection. In *European Conference on Computer Vision*, 2020.

[Qiu *et al.*, 2021] Han Qiu, Yi Zeng, Shangwei Guo, Tianwei Zhang, Meikang Qiu, and Bhavani Thuraisingham. Deepsweep: An evaluation framework for mitigating dnn backdoor attacks using data augmentation. In *ACM Asia Conference on Computer and Communications Security*, 2021.

[Quiring and Rieck, 2020] Erwin Quiring and Konrad Rieck. Backdooring and poisoning neural networks with image-scaling attacks. In *IEEE Security and Privacy Workshops*, 2020.

[Quiring *et al.*, 2020] Erwin Quiring, David Klein, Daniel Arp, Martin Johns, and Konrad Rieck. Adversarial pre-processing: Understanding and preventing image-scaling attacks in machine learning. In *USENIX Security Symposium*, 2020.

[Raj *et al.*, 2021] Ankita Raj, Ambar Pal, and Chetan Arora. Identifying physically realizable triggers for backdoored face recognition networks. In *IEEE International Conference on Image Processing*, 2021.

[Sato *et al.*, 2021] Takami Sato, Junjie Shen, Ningfei Wang, Yunhan Jia, Xue Lin, and Qi Alfred Chen. Dirty road can attack: Security of deep learning based automated lane centering under {Physical-World} attack. In *USENIX Security Symposium*, 2021.

[Shafahi *et al.*, 2018] Ali Shafahi, W Ronny Huang, Mahyar Najibi, Octavian Suciu, Christoph Studer, Tudor Dumitras, and Tom Goldstein. Poison frogs! targeted clean-label poisoning attacks on neural networks. *arXiv preprint arXiv:1804.00792*, 2018.

[Tabelini *et al.*, 2021a] Lucas Tabelini, Rodrigo Berriel, Thiago M Paixao, Claudine Badue, Alberto F De Souza, and Thiago Oliveira-Santos. Keep your eyes on the lane: Real-time attention-guided lane detection. In *IEEE/CVF Conference on Computer Vision and Pattern Recognition*, 2021.

[Tabelini *et al.*, 2021b] Lucas Tabelini, Rodrigo Berriel, Thiago M Paixao, Claudine Badue, Alberto F De Souza, and Thiago Oliveira-Santos. Polylanenet: Lane estimation via deep polynomial regression. In *International Conference on Pattern Recognition*, 2021.

[Wang *et al.*, 2019] Bolun Wang, Yuanshun Yao, Shawn Shan, Huiying Li, Bimal Viswanath, Haitao Zheng, and Ben Y Zhao. Neural cleanse: Identifying and mitigating backdoor attacks in neural networks. In *IEEE Symposium on Security and Privacy*, 2019.

[Wenger *et al.*, 2021] Emily Wenger, Josephine Passananti, Arjun Nitin Bhagoji, Yuanshun Yao, Haitao Zheng, and Ben Y Zhao. Backdoor attacks against deep learning systems in the physical world. In *IEEE/CVF Conference on Computer Vision and Pattern Recognition*, 2021.

[Xiao *et al.*, 2019] Qixue Xiao, Yufei Chen, Chao Shen, Yu Chen, and Kang Li. Seeing is not believing: Camouflage attacks on image scaling algorithms. In *USENIX Security Symposium*, 2019.

[Xue *et al.*, 2021] Mingfu Xue, Can He, Shichang Sun, Jian Wang, and Weiqiang Liu. Robust backdoor attacks against deep neural networks in real physical world. *arXiv preprint arXiv:2104.07395*, 2021.

[Zhao *et al.*, 2020] Shihao Zhao, Xingjun Ma, Xiang Zheng, James Bailey, Jingjing Chen, and Yu-Gang Jiang. Clean-label backdoor attacks on video recognition models. In *IEEE/CVF Conference on Computer Vision and Pattern Recognition*, 2020.

A Appendix

In this section, we show more experimental details and additional results of our two attacks: poison-annotation attack and clean-annotation attack. The four models' official source codes can be found in **Tusimple Lane Detection Challenge**². For more details of our attack implementation, the source code will be published soon.

A.1 Poison-annotation Attacks

Figure 11 shows generated examples by normal and (20, 40, 60, 80, 100) backdoored models. The first row shows the injected trigger does not affect the prediction of four backdoor-free models. This indicates the robustness of the four models. Nevertheless, the four models are severely affected by poison-annotation attacks as the triggered images increase, as shown.

To evaluate the effectiveness of the poison-annotation backdoor attacks, we compare the ASR computed by our accuracy metric given in Eqn. 4 with that computed by a conventional accuracy metric, which is defined as:

$$\text{acc}(M, s) = \frac{\sum_i^n \text{acc}(\bar{l}_i, l_i)}{n} \quad (9)$$

Figure 12 shows the ASR computed by Eqn.9. Compared with results given in Figures 6, we can conclude that the conventional accuracy metric cannot truly reflect the attack performance.

A.2 Clean-annotation Attacks

Figure 13 shows generated examples under clean-annotation attack with L2R and R2L by four backdoored models.

A.3 Evaluation in Real-World

We evaluated our two types of attacks on a right-turn lane and straight lane scenarios on campus. Despite the huge gap between simulation and real-world scenarios, the lane detection models are still able to differentiate the ego lane boundaries, our attacks also exhibit strong transferability and practicality. Figure 14 shows the generated normal and (20, 40, 60, 80, 100) attacked examples at a straight lane with SCNN. As shown, we can get the same conclusion from Section A.1 that a larger poisoning ratio leads to more noticeable attack effects.

Figure 15 shows the examples generated by SCNN under clean-annotation attack at a right-turn lane. We placed the trigger at 7 meters in front of the UGV since this is the safety braking distance at 25 mph in normal driving. Nevertheless, our attack is still effective at less than seven meters, as demonstrated in Figure 15 (a) and (b).

A.4 Defense

We give the details of implementations and results of **Fine-Pruning** and **Median-Filtering** on two attacks with SCNN.

In the setting of Fine-Pruning, we pruning layer1 in SCNN model. The layer1 connects the feature extraction layer with four significant layers in SCNN named: up_down layer,

down_up layer, left_right layer, and right_left layer. The number of neurons in layer1 is 1024. We pruning the number of neurons from 0 until the model accuracy drop dramatically, the interval is set as 100. Table 4 gives the defense results against poison-annotation attack. Same with what we discussed in Table 2, fine-pruning is inefficient against our attacks.

In the setting of Median-Filtering, we analyze the recovery of an attack image generated by a source image with 1280*720 and a triggered target image with 320*180. The results are shown in Figure 16. From the results, we can find that the attacked image (Figure 16(b)) shows a similar histogram with the original one (Figure 16(a)). Note that after the deployment of the model, the user has no knowledge of the original images of the attacked ones, he/she can only obtain the histograms of the attacked and the restored images. However, from Figures 16(b) and 16(c), they have no significant difference in the histogram. What's more, as discussed in section 4.4, the restored image still remains the physical trigger.

²<https://paperswithcode.com/sota/lane-detection-on-tusimple>

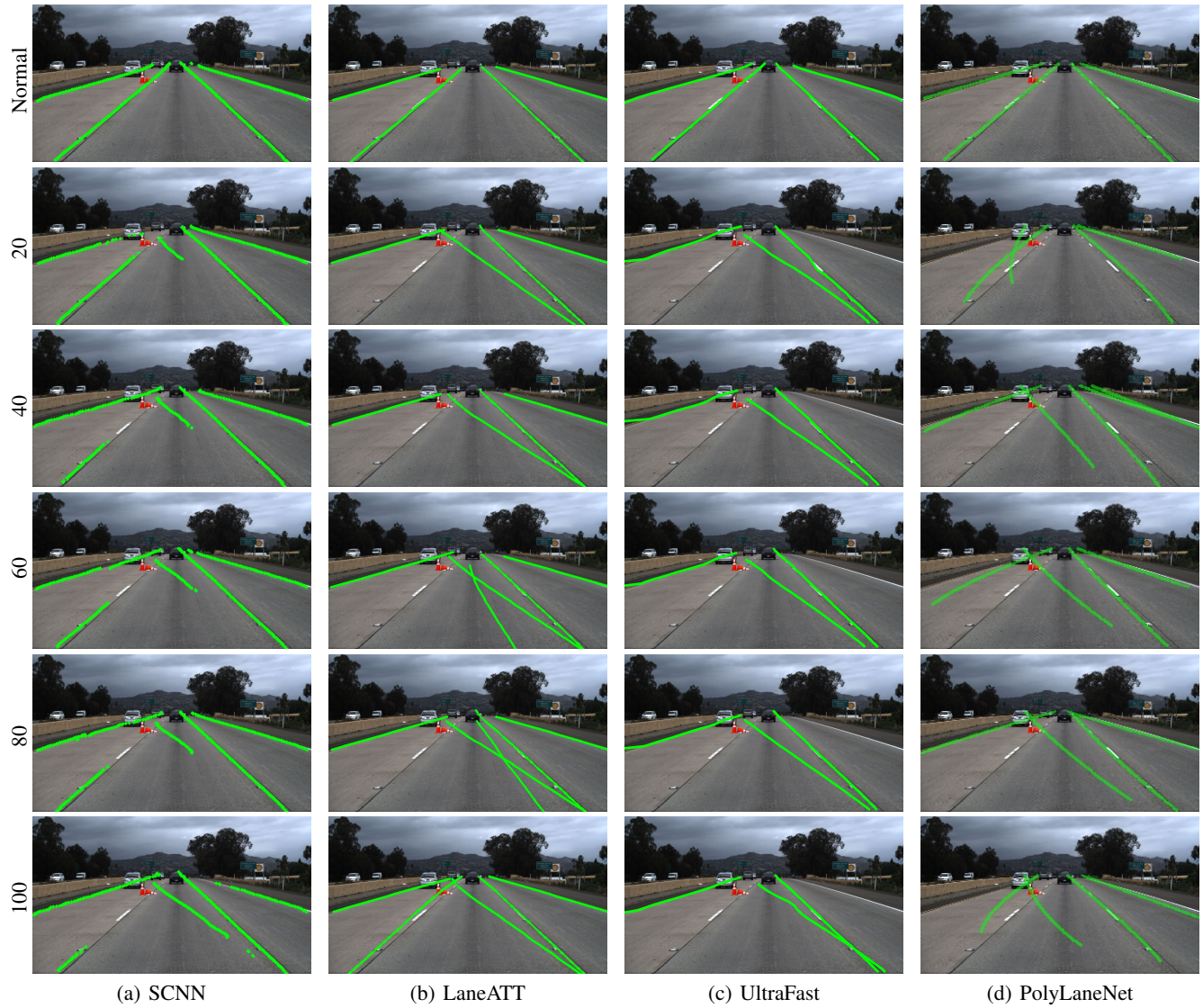


Figure 11: Generated example under poison-annotation attack on Tusimple with different number of poisoned images.

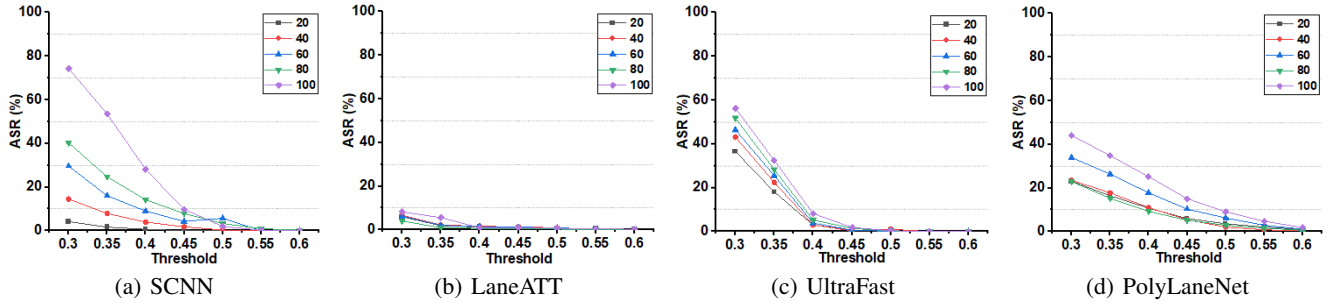


Figure 12: The ASR computed according to Eqn. 9 with different thresholds.

SCNN		LaneATT		UltraFast		PolyLaneNet		
acc normal (%)	acc poisoned (%)	acc normal (%)	acc poisoned (%)	acc normal (%)	acc poisoned (%)	acc normal (%)	acc poisoned (%)	
0	94.41	94.41	95.38	95.38	95.82	95.82	89.77	89.77
20	93.81	86.98	95.49	76.49	95.65	71.61	89.41	75.3
40	94.06	81.97	94.93	76.19	95.79	70.41	89.94	76.83
60	92.9	77.05	95.21	76.04	95.66	69.72	89.26	71.16
80	94.03	77.02	95.57	76.03	95.66	68.86	88.76	75.76
100	92.6	70.97	95.59	75.79	95.54	67.91	87.81	66.31

Table 3: The detailed accuracy of Fig 5.

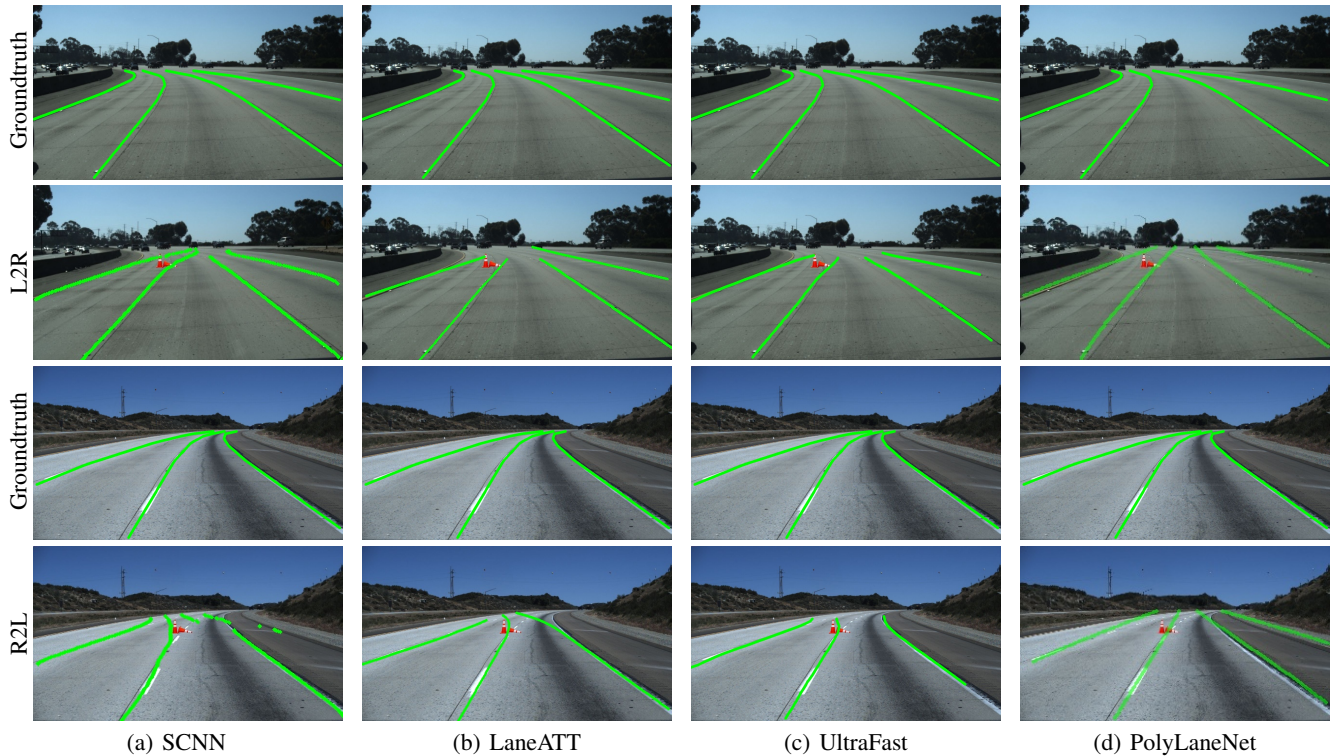


Figure 13: Generated examples under clean-annotation attack on Tusimple with L2R and R2L effects.

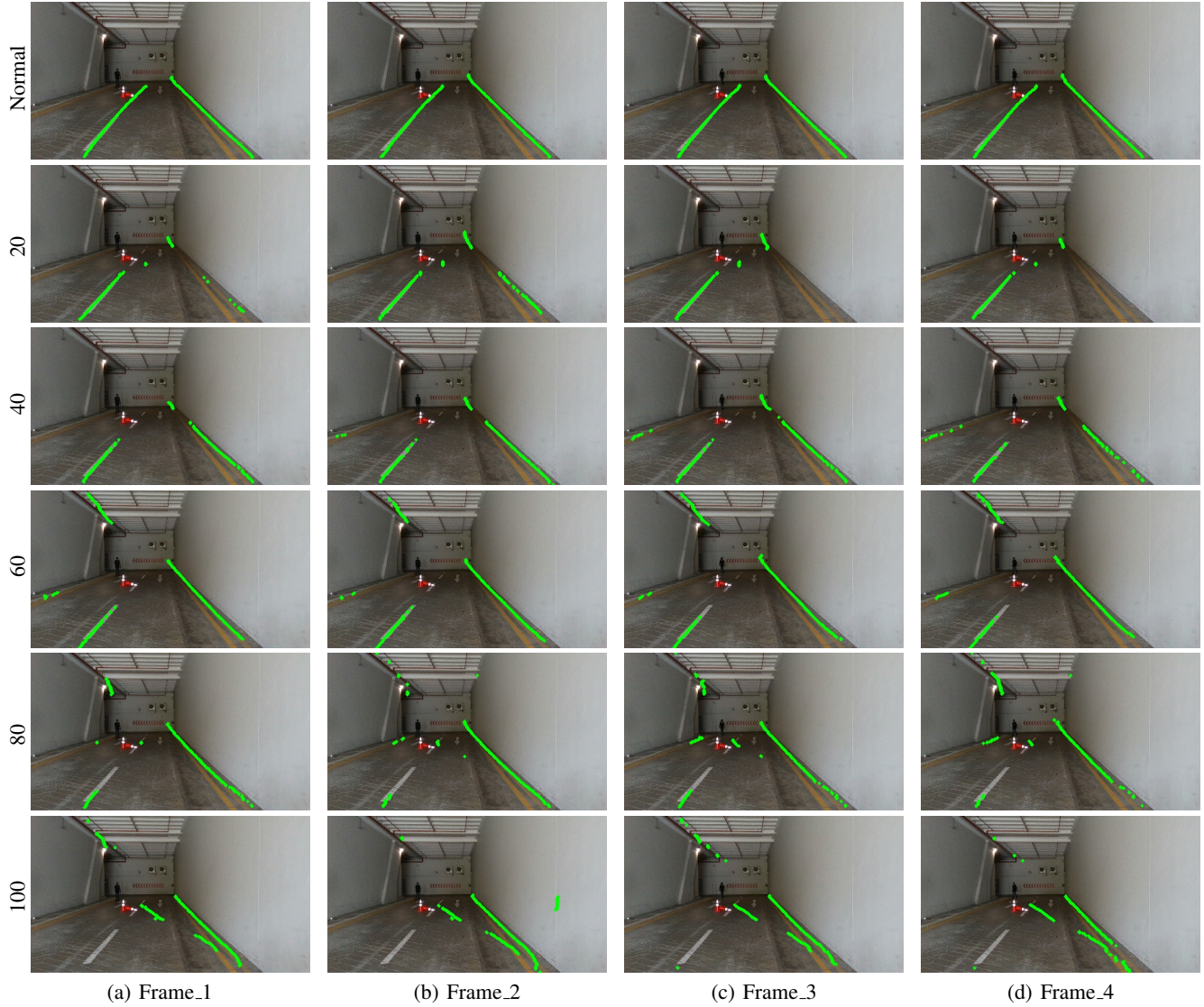


Figure 14: Poison-annotation attacks evaluated in the real-world (SCNN). Each column represents a frame at a certain second.

Remove cells	0	50	100	150	200	250	300	350	400
Normal ACC (%)	94.40	94.45	94.46	94.04	93.59	92.45	88.21	84.63	77.70
Poisoned ACC (%)	70.47	70.53	70.34	70.66	70.34	69.51	67.07	66.54	63.35

Table 4: Fine-pruning defense against poison-annotation attack (SCNN).

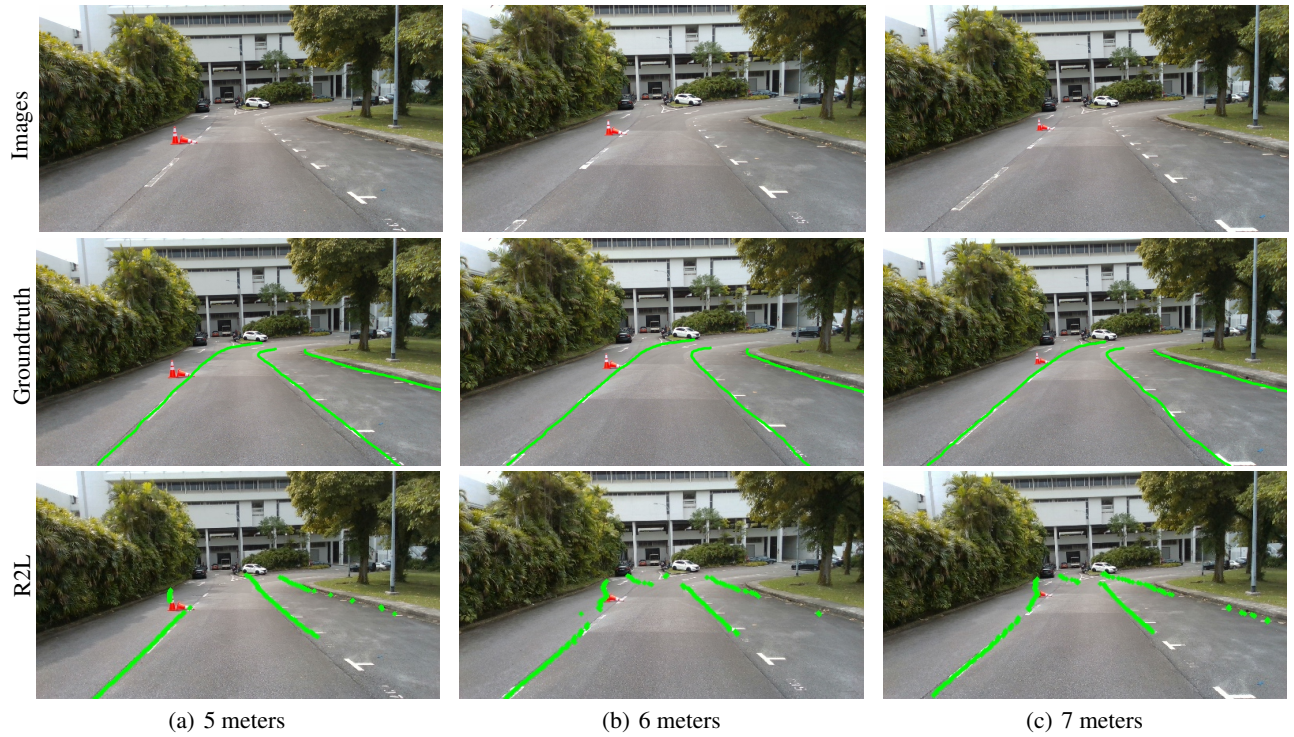


Figure 15: Clean-annotation attacks evaluated in physical world with different distances between trigger and camera (SCNN).

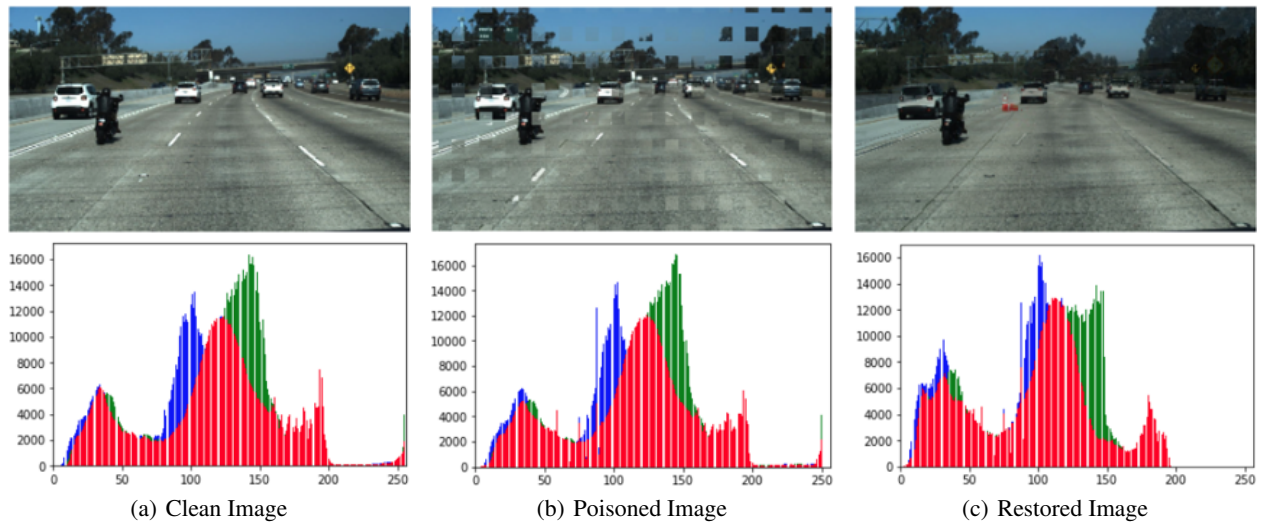


Figure 16: The analysis of median filtering defense.